Integration of Subretinal Suspension Transplants of Human Embryonic Stem Cell-Derived Retinal Pigment Epithelial Cells in a Large-Eyed Model of Geographic Atrophy

Sandra Petrus-Reurer,[1,2] Hammurabi Bartuma,[1] Monica Aronsson,[1] Sofie Westman,[1] Fredrik Lanner,[2] Helder André,[1] and Anders Kvanta[1]

[1]Department of Clinical Neuroscience, Section for Ophthalmology and Vision, St. Erik Eye Hospital, Karolinska Institutet, Stockholm, Sweden
[2]Department of Clinical Sciences, Intervention and Technology, Karolinska Institutet, Stockholm, Sweden and Division of Obstetrics and Gynecology, Karolinska University Hospital, Stockholm, Sweden

Correspondence: Anders Kvanta, St. Erik Eye Hospital and Karolinska Institutet, Polhemsgatan 50, SE11282 Stockholm, Sweden; anders.kvanta@ki.se.

SP-R and HB contributed equally to the work presented here and should therefore be regarded as equivalent authors.

Submitted: September 12, 2016
Accepted: January 23, 2017

Citation: Petrus-Reurer S, Bartuma H, Aronsson M, et al. Integration of subretinal suspension transplants of human embryonic stem cell-derived retinal pigment epithelial cells in a large-eyed model of geographic atrophy. *Invest Ophthalmol Vis Sci*. 2017;58:1314–1322. DOI:10.1167/iovs.16-20738

Purpose. Subretinal suspension transplants of human embryonic stem cell-derived retinal pigment epithelial cells (hESC-RPE) have the capacity to form functional monolayers in naive eyes. We explore hESC-RPE integration when transplanted in suspension to a large-eyed model of geographic atrophy (GA).

Methods. Derivation of hESC-RPE was performed in a xeno-free and defined manner. Subretinal bleb injection of PBS or sodium iodate ($NaIO_3$) was used to induce a GA-like phenotype. Suspensions of hESC-RPE were transplanted to the subretinal space of naive or PBS-/$NaIO_3$-treated rabbits using a transvitreal pars plana technique. Integration of hESC-RPE was monitored by multimodal real-time imaging and by immunohistochemistry.

Results. Subretinal blebs of PBS or $NaIO_3$ caused different degrees of outer neuroretinal degeneration, RPE hyperautofluorescence, focal RPE loss, and choroidal atrophy; that is, hallmark characteristics of GA. In nonpretreated naive eyes, hESC-RPE integrated as subretinal monolayers with preserved overlying photoreceptors, yet not in areas with outer neuroretinal degeneration and native RPE loss. When transplanted to eyes with PBS-/$NaIO_3$-induced degeneration, hESC-RPE failed to integrate.

Conclusions. In a large-eyed preclinical model, subretinal suspension transplants of hESC-RPE did not integrate in areas with GA-like degeneration.

Keywords: preclinical model, embryonic stem cells, retinal pigment epithelium, photoreceptor, phosphate-buffered saline, sodium iodate, real-time imaging

Cell replacement therapy using retinal pigment epithelial cells (RPE) derived from human embryonic stem cells (hESC) for geographic atrophy (GA), the advanced form of dry age-related macular degeneration (AMD), and related disease currently is being explored in pilot clinical trials.[1,2] Preliminary results have confirmed the safety of this approach, yet efficacy data, including functional integration of transplanted cells, have not yet been demonstrated. Also, preclinical data have been limited largely to small-eyed rodents that do not capture vital aspects of surgical intervention of human GA.[3,4] In GA, the native RPE degenerate resulting in collateral atrophy of the overlying photoreceptors and the underlying choriocapillaris.[5,6] In addition, Bruch's membrane, the basal membrane of the RPE, undergoes age-related changes during disease progression that in turn may limit integration of suspension transplants.[7,8] Consequently, transplantation of hESC-RPE monolayers on a supportive biomatrix has been proposed.[9,10] Since optimal integration of transplanted hESC-RPE is critical for a fully successful regenerative treatment of GA, it is vital that integration issues are carefully explored in a relevant large-eyed preclinical model.[11]

We recently demonstrated that subretinal bleb injections of physiologic salt solutions in the large-eyed rabbit cause robust photoreceptor loss and RPE alterations; that is, hallmark features of clinical GA.[12] We have shown further that subretinal suspension transplants of hESC-RPE derived in a xeno-free and defined manner on laminin (LN)-521, a component of Bruch's membrane, integrate as pigmented and functional monolayers, including phagocytic and photoreceptor rescue capacity.[13] We also reported that integration success varied between eyes, and postulated that such variability could be dependent partly on the degree of bleb-associated outer neuroretinal and RPE damage. To further address this, we analyzed how hESC-RPE suspension transplants integrate in eyes with preinduced GA-like photoreceptor and RPE damage using either PBS or sodium iodate ($NaIO_3$).

Materials and Methods

Cell Culture

The human embryonic stem cell line HS980 was derived and cultured under xeno-free and defined conditions as described previously.[9,14] Cells were maintained by clonal propagation on human recombinant LN-521 (10 μg/mL, Biolamina, Sundbyberg, Sweden) in NutriStem hESC XF medium (Biological

Table 1. Summary of Eyes Treated and Examined in the Study

Treatment	Eyes Treated, *n*	Eyes Included, *n**
PBS	16	14†
$NaIO_3$	14	14
hESC-RPE	12	12
PBS + hESC-RPE	12	5‡
$NaIO_3$ + hESC-RPE	12	5‡

* Eyes eligible for multimodal imaging.

† Eyes were excluded if BAF images could not be obtained.

‡ Eyes were included if multimodal imaging could be obtained before and 3 months after transplantation. Eyes were excluded if second bleb was not formed or was formed outside of the first bleb, or if signs of immunorejection was detected (i.e., subretinal infiltration with choroidal swelling on SD-OCT).

Industries, Cromwell, CT, USA), in a 5% CO_2/5% O_2 incubator and passaged enzymatically at 1:10 ratio every 5 to 6 days: confluent cultures were washed twice with PBS without Ca^{2+} and Mg^{2+} and incubated for 5 minutes at 37°C, 5% CO_2/5% O_2 with TrypLE Select (Thermo Fisher Scientific, Waltham, MA, USA). TrypLE Select then was carefully removed and the cells were collected in fresh prewarmed NutriStem hESC XF medium by gentle pipetting to obtain a single cell suspension. Cells were centrifuged at 200*g* for 4 minutes and the pellet was resuspended in fresh prewarmed NutriStem hESC XF medium and plated on a freshly LN-521 coated dish. Two days after passage the medium was replaced with fresh prewarmed NutriStem hESC XF medium and changed daily.

In Vitro Differentiation

Pluripotent stem cells were cultured to confluence on LN-521 and manually scraped to produce embryoid bodies (EBs) using a 1000 µl pipette tip as described previously.[13] Embryoid bodies were cultured in suspension in low attachment plates (Corning, Corning, NY, USA) at a density of 5 to 7 × 10^4 cells/cm^2. Differentiation of RPE from hESC was performed by the removal of bFGF and TGFβ from a custom-made NutriStem hESC XF media and the addition of 10 µM Rho-kinase inhibitor (Y-27632; Merck Millipore, Billerica, MA, USA) to the suspension cultures exclusively during the first 24 hours. Media then was changed twice a week. After 5 weeks of differentiation, pigmented areas were mechanically cut out of the EBs using a scalpel. Cells were dissociated using TrypLE Select, pushed through a 20 G needle and a cell strainer (ø 40 µm; BD Biosciences, San Jose, CA, USA), and seeded on LN-521-coated dishes (20 µg/mL; Biolamina) at a cell density of 0.6 to 1.2 × 10^4 cells/cm^2. Cell culture medium was changed twice a week with the same differentiation medium as above.

Animals

After approval by the Northern Stockholm Animal Experimental Ethics Committee, 33 New Zealand white albino rabbits (provided by Lidköpings rabbit farm, Lidköping, Sweden) aged 5 months, weighing 3.5 to 4.0 kg, were used in this study (Table 1). All experiments were conducted in accordance with the ARVO Statement for the Use of Animals in Ophthalmic and Vision Research.

Subretinal Injection

Animals were anesthetized by intramuscular administration of 35 mg/kg ketamine (Ketaminol, 100 mg/ml; Intervet, Boxmeer, The Netherlands) and 5 mg/kg xylazine (Rompun vet. 20 mg/ml; Bayer Animal Health, Leverkusen, Germany), and the pupils were dilated with a mix of 0.75% cyclopentolate and 2.5% phenylephrine (APL, Stockholm, Sweden). Microsurgeries were performed on both eyes as previously described using a 3-port 25 G transvitreal pars plana technique (Alcon Accurus; Alcon Nordic, Copenhagen, Denmark).[12] Phosphate buffered saline (Thermo Fisher Scientific) or $NaIO_3$ (Sigma-Aldrich Corp., St. Louis, MO, USA) in PBS was drawn into a 1 mL syringe connected to an extension tube (operated by the assistant) and a 38 G polytip cannula (operated by the surgeon; MedOne Surgical, Inc., Sarasota, FL, USA). Then, 25 G trocars were inserted 1 mm from the limbus and an infusion cannula was connected to the lower temporal trocar. Without infusion or prior vitrectomy, the cannula was inserted through the upper temporal trocar and the tip of the cannula was allowed to slowly penetrate the retina just below the optic nerve head. After proper tip positioning, ascertained by a focal whitening of the retina, 50 µL of PBS or indicated doses of $NaIO_3$ were injected slowly subretinally, forming a uniform semitransparent bleb that was clearly visible under the operating microscope. Care was taken to maintain the tip within the bleb during the injection to minimize reflux. After instrument removal, light pressure was applied to the self-sealing suture-less sclerotomies. No postsurgical topical steroids or antibiotics were given. On postsurgical follow-up, none of the eyes showed signs of extra- or intraocular infection or inflammation. Relative areas of hypoautofluorescence were measured manually on blue-light autofluorescence (BAF) images obtained 4 to 6 months after injection using ImageJ software (http://imagej.nih.gov/ij/; provided in the public domain by the National Institutes of Health, Bethesda, MD, USA).

Subretinal Transplantation

Subretinal suspension transplantations of hESC-RPE were performed as previously described.[13] Monolayers of hESC-RPE were washed with PBS, incubated with TrypLE and dissociated to single cell suspension. Cells were counted in a Neubauer hemocytometer chamber using 0.4% trypan blue (Thermo Fisher Scientific), centrifuged at 300*g* for 4 minutes, and the cell pellet was resuspended in freshly filter-sterilized PBS to a final concentration of 1000 cells/µL. The cell suspension then was aseptically aliquoted into 600 µL units and kept on ice until surgery.

Animals were anesthetized and prepared for surgery as described in "Subretinal Injection." After proper tip positioning, ascertained by a focal whitening of the retina, an equivalent of 50,000 cells (50 µL of cell suspension) was injected subretinally below the optic nerve head. Phosphate buffered saline or $NaIO_3$ pretreated areas were distinguished by a characteristic "metallic" endo-illumination reflex and reinjection by hESC-RPE was performed in the center of this area. In most cases, the neurosensory retina separated easily creating clearly visible blebs that, in contrast to naïve blebs, were almost transparent. Care was taken to maintain the tip within the bleb during the injection to minimize reflux. After instrument removal light pressure was applied to the self-sealing suture-less sclerotomies. Immunosuppression of hESC-RPE transplanted animals was done with 2 mg (100 µL) of intravitreal triamcinolone (Triescence; Alcon Nordic) 1 week before transplantation and was readministered every 3 months as described previously.[13]

Multimodal Real-Time Imaging

All treated rabbits were examined at regular intervals (i.e., 1, 4, 12, 26 weeks) with real-time multimodal imaging for up to 6 months. Anesthetized animals were placed in an adjustable

mount. A commercial Spectralis HRA + OCT device (Heidelberg Engineering, Heidelberg, Germany) with the Heidelberg Eye Explorer Software (version 1.9.10.0) was used to obtain horizontal cross-sectional b-scans of treated animals. At least 3 cross-sectional spectral domain-optical coherence tomography (SD-OCT) scans were obtained with simultaneous infrared-confocal scanning laser ophthalmoscope (IR-cSLO) reflectance reference images representing the upper, central, and lower portions of the treated area. The best overall image quality was obtained when the OCT setting was on high-speed acquisition with at least 50 averaged automatic real-time images. En face fundus images were obtained by IR- or multicolor cSLO (a composite of three simultaneously acquired color cSLO images). These modalities have a higher contrast level compared to conventional fundus camera photos. In addition, corresponding BAF images were captured using the Spectralis blue light-laser with an excitation wavelength of 488 nm and a barrier filter of 500 nm.

Histology and Tissue Immunostaining

Animal euthanasia and enucleation was performed as described previously.[12] For immunostaining, slides were deparaffinized in xylene, dehydrated in graded alcohols, and rinsed with dH_2O and Tris-buffered saline (TBS, pH 7.6). Then, 10 mM citrate buffer (trisodium citrate dehydrate, pH 6.0; Sigma-Aldrich Corp.) with 0.05% Tween-20 (Sigma-Aldrich Corp.) at 96°C for 30 minutes, followed by 30 minutes of cooling at room temperature was used as antigen retrieval method. Slides were washed with TBS and blocked for 30 minutes in a humidified chamber in a mix of normal protease-free sera (10% normal donkey serum (Abcam, Cambridge, United Kingdom) and 5% (wt/vol) protease free bovine serum albumin (Jackson Immunoresearch Labs, West Grove, PA, USA) diluted in TBS. Primary antibodies (human nuclear mitotic apparatus protein [NuMA; 1:200; Abcam ab84680) and RPE65 (1:100; Merck Millipore MAB5428) were diluted in blocking buffer and were incubated overnight at 4°C. Secondary antibodies (Alexa Fluor 555 donkey anti-rabbit IgG A31572 and Alexa Fluor 647 donkey anti-mouse IgG A31571 or Alexa Fluor 555 donkey anti-mouse IgG A31570, all from Life Technologies, Carlsbad, CA, USA) were diluted 1:200 in blocking buffer and incubated 1 hour at room temperature. Sections were mounted with Vectashield with 4′,6-diamidino-2-phenylendole (DAPI) mounting medium (Vector Laboratories, Burlingame, CA, USA) in a 24 × 50 mm coverslip. Images were acquired with a Zeiss LSM710-NLO point scanning confocal microscope and Olympus IX81 fluorescence microscope (Carl Zeiss Meditec, Jena, Germany). Post-acquisition analysis of the pictures was performed using ImageJ software.

Immunofluorescence

Cells were fixed with 4% methanol free formaldehyde at room temperature for 20 minutes, followed by permeabilization with 0.3% Triton X-100 in Dulbecco's PBS (DPBS) for 10 minutes and blocking with 4% fetal bovine serum (FBS) and 0.1% Tween-20 in DPBS for 1 hour. RPE65 antibody (Abcam ab78036, clone [401.8B11.3D9]) was diluted 1:200 in DPBS solution with 4% FBS and 0.1% Tween-20 overnight at 4°C, followed by 2 hours incubation at room temperature with secondary antibody Alexa Fluor 555 donkey anti-mouse IgG (1:1000, Life Technologies, A31570) in DPBS solution with 4% FBS, 0.1% Tween-20. Nuclei were stained with Hoechst 33342 (1:1000; Invitrogen, Carlsbad, CA, USA). Images were acquired with a Zeiss LSM710-NLO point scanning confocal microscope. Postacquisition analysis of the pictures was performed using ImageJ software.

Statistical Analysis

For statistical analyses, the independent Student's *t*-test and χ^2 test were used to compare differences in hypo-BAF areas and incidence of RPE atrophy between PBS- or $NaIO_3$-treated groups.

Results

Induction of a GA-Like Phenotype by Subretinal PBS and $NaIO_3$

In the large-eyed rabbit, we have shown previously that subretinal blebs of PBS cause hyper- and hypo-BAF of the RPE that persist for up to 1 month and photoreceptor loss that progressed for up to 3 months.[12] Extending the observation time for up to 6 months, the observed changes to the outer neuroretina/RPE complex persisted and even became more pronounced (Fig. 1A). Notably, the hyper-BAF zone showed increased intensity through time. We also observed further loss of outer retinal layers, including the inner plexiform layer in areas of hypo-BAF by SD-OCT (Fig. 1A). On histology, the transition between the hyper- and hypo-BAF zones was clearly distinguishable (Fig. 1B). Immunostaining for the RPE marker, RPE65, confirmed presence of native RPE in the hyper- but not in the hypo-BAF zone (Fig. 1C). These RPE denuded areas showed severe retinal atrophy, including a complete loss of photoreceptor nuclei and fusion with the underlying structures. Thus, subretinal bleb injection of PBS alone can induce a long-term GA-like phenotype. However, in contrast to photoreceptor loss and hyper-BAF that were observed in all PBS-treated eyes, the presence of hypo-BAF areas were rare (Table 2). Since a main objective of this study was to examine how hESC-RPE suspensions may integrate in eyes with GA-like changes, we, thus, sought to adopt a large-eyed model that more specifically targeted the RPE.

Sodium iodate has been shown previously to induce RPE and outer neuroretinal degeneration in various animal models, including rabbit.[15–17] In these studies, the toxin was administered systemically resulting in patchy panretinal degeneration. To better mimic clinical GA we sought to explore subretinal administration of $NaIO_3$. Subretinal $NaIO_3$ blebs resulted in a dose-dependent degeneration of the outer neuroretina and RPE (Fig. 2A; Supplementary Fig. S1). A dose of 0.1 mM $NaIO_3$ caused changes similar to PBS alone with hyper-BAF within the bleb area. On SD-OCT, the ellipsoid zone and outer limiting membrane bands were lost and the outer nuclear layer thinned. At higher doses (1 and 10 mM) the $NaIO_3$-induced damage became more pronounced with large areas of RPE degeneration (i.e., hypo-BAF) accompanied by progressive loss of outer neuroretinal layers on SD-OCT. At 1 mM of $NaIO_3$ the entire outer nuclear layer was lost, whereas a dose of 10 mM also caused a loss of the inner plexiform layer. In normal eyes, the RPE/Bruch's/choriocapillary layer was clearly distinguishable on SD-OCT as we have reported previously.[12,13] Following $NaIO_3$ treatment, a dose-dependent thinning of this layer was observed further supporting RPE loss (Fig. 2). In addition, a marked dose-dependent thinning of the choroidal layer was noted on SD-OCT (Supplementary Fig. S1). On histology, the area of RPE loss showed fusion of the atrophic neuroretina to the underlying structures similar to areas of PBS-induced RPE loss (Fig. 2B, Supplementary Fig. S1). However, when comparing the frequency and area of RPE loss, we found a statistically significant difference between PBS- and 1 mM $NaIO_3$-injected eyes (Table 2). Together, our data show that subretinal injection of medium (1 mM) and high (10 mM) doses of $NaIO_3$ induces degeneration of the neuroretina/RPE/choroid

Investigative Ophthalmology & Visual Science

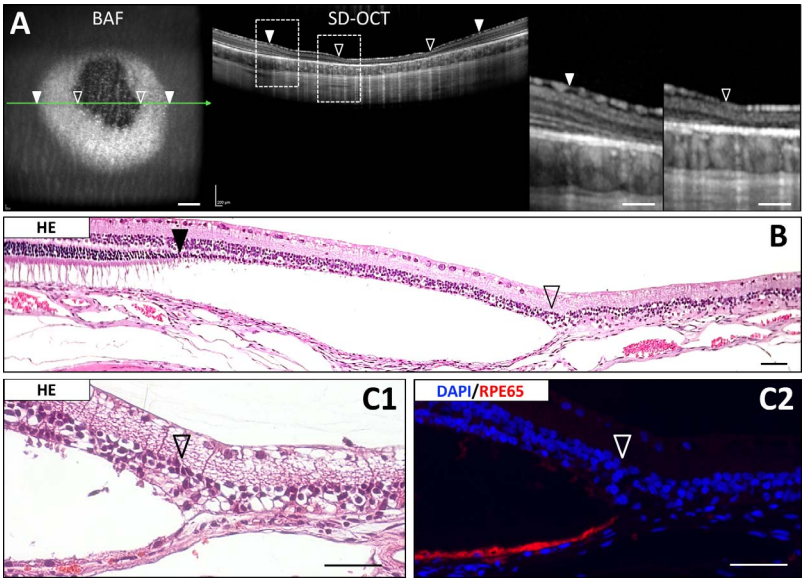

Figure 1. Subretinal PBS induces a GA-like phenotype. Phosphate buffered saline-induced subretinal damage in albino rabbits imaged by BAF and SD-OCT (**A**). The SD-OCT scan plane is marked (*green arrow*). The RPE layer displays a hypo-BAF center area surrounded by a hyper-BAF rim 4 months after PBS injection. The transition from normal to rim area (*closed arrowhead*) and from rim to center area (*open arrowhead*) is marked. On SD-OCT the rim area (hyper-BAF) demonstrates loss of the ellipsoid zone and outer limiting membrane bands with thinning of the outer nuclear layer whereas the center area (hypo-BAF) exhibits loss of the outer nuclear and inner plexiform layers. *Boxes* show magnifications of the rim and center areas (*right panels*). The rim and center areas are clearly distinguished on the corresponding HE stained histologic section (**B**). In the *rim area* the photoreceptors are reduced to a single layer whereas the *center area* shows further neuroretinal atrophy and fusion with the underlying structures. Hematoxylin and eosin (HE; [**C1**]) and immunostaining (**C2**) for RPE65 demonstrates loss of native RPE in the center area. *Scale bars*: (**A**) 200 μm; (**B**, **C**) 50 μm.

complex similar to clinical GA and in a more consistent manner than PBS.

Transplantation of hESC-RPE in Naive and PBS- or $NaIO_3$-Pretreated Eyes

Derivation of hESC-RPE was done on LN-521 according to our previously described xeno-free and defined protocol.[13] Hexagonal monolayers showed gradual pigmentation and RPE65 cytoplasmic-membrane expression during differentiation toward mature RPE (Fig. 3A). After suspension transplantation in nonpretreated naive eyes, hESC-RPE could form extensive pigmented subretinal monolayers that were constantly and continually in the correct position between the photoreceptors and Bruch's membrane, and never overlaying the native RPE. As expected, the native nonpigmented RPE was overall strongly positive for RPE65. Surprisingly, hESC-RPE initially failed to express RPE65, yet regained expression gradually, becoming immunopositive through time (Figs. 3B, 3C). Importantly, in naive eyes hESC-RPE were not found in areas of outer neuroretinal degeneration and native RPE loss (Fig. 4A). Nevertheless, adjacent areas where hESC-RPE successfully integrated were overlaid with well-preserved photoreceptor nuclei and outer segments.

To address whether hESC-RPE also could integrate in areas with GA-like damage, cells were transplanted to PBS- and $NaIO_3$-pretreated eyes. On follow-up, we noted that some secondary blebs had formed outside and not within the first bleb. In addition, and in contrast to hESC-RPE transplants in nonpretreated naive eyes, signs of immunorejection (i.e., SD-OCT verified subretinal infiltration and choroidal swelling) were observed in one PBS- and two $NaIO_3$-pretreated eyes that were consequently excluded from further analysis (Table 3).

One week after PBS pretreatment, suspension transplantations of hESC-RPE were performed. Spectral domain-OCT and BAF images taken before transplantation confirmed loss of photoreceptor layers and presence of hyper-BAF (Table 3). After 3 months of follow-up, occasional pigmented dots, but no confluent layers, were detected in the bleb area by cSLO (Fig. 4B). Spectral domain-OCT confirmed the presence of small hyperreflective patches indicative of donor cells. On histology and immunostaining, these areas were found to contain occasional pigmented RPE65–positive cells with aberrant morphology (Fig. 4B). For $NaIO_3$ pretreatment, we selected a dose of 1 mM and similarly performed bleb injections 1 week before transplantation with hESC-RPE suspensions. Spectral domain-OCT and BAF images of the blebs before reinjection with hESC-RPE confirmed loss of photoreceptor layers and presence of hyper- and hypo-BAF (Fig. 4C; Table 3). On follow-up, integration of hESC-RPE was not observed by either cSLO or SD-OCT after 3 months (Fig. 4C). Collectively, we found no evidence that hESC-RPE in suspension could integrate in the

Table 2. PBS- and $NaIO_3$-Induced RPE Atrophy

Treatment	Eyes Included, *n*	RPE Atrophy, *n**	*P* Value†	Atrophy Area, % (Range)‡	*P* Value§
PBS	14	5		3.4 (0–26.1)	
$NaIO_3$	12	8	0.007	16.9 (0–46.0)	0.004

* Hypo-BAF area.
† χ^2 test for PBS versus 1 mM $NaIO_3$.
‡ Mean ratio of hypo-BAF area and total bleb area.
§ Unpaired 2-tailed Student's *t*-test for PBS versus 1 mM $NaIO_3$.

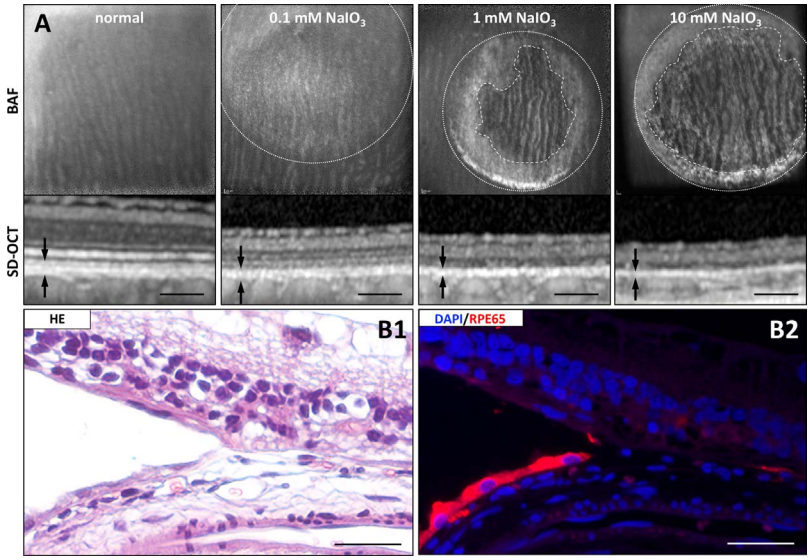

Figure 2. Subretinal injection of $NaIO_3$ induces dose-dependent GA-like phenotype. Subretinal injection of $NaIO_3$ induces dose-dependent RPE degeneration as demonstrated by BAF after 3 months (**A**). The corresponding SD-OCT image is shown below. At a dose of 0.1 mM $NaIO_3$ the effect was similar to PBS alone demonstrating hyper-BAF in the bleb area (*dotted circle*) and corresponding loss of the outermost neuroretinal layers on SD-OCT. At a dose of 1 mM $NaIO_3$, a hypo-BAF area (*dashed line*) covering a large portion of the bleb was observed. At the highest dose (10 mM) the hypo-BAF area covered the vast majority of the bleb. Spectral domain-OCT showed absolute loss of the outer nuclear layer with 1 mM $NaIO_3$, whereas the 10 mM dose also resulted in loss of the inner plexiform layer. Note also the marked thinning of the RPE/Bruch's/choriocapillaris layer with higher $NaIO_3$ doses (*between arrows*). HE (**B1**) and immunostaining (**B2**) of the hyper-/hypo-BAF transition zone confirmed loss of RPE65-positive native RPE and fusion of the atrophic neuroretina to the underlying structures (**B**). *Scale bars*: (**A**) 200 μm; (**B**) 20 μm.

area of preinduced degeneration of the outer neuroretina/RPE complex, in either PBS- or $NaIO_3$-pretreated eyes.

Overall, these findings demonstrated that a well-conserved outer neuroretina/RPE complex is fundamental for effective integration of a donor source of hESC-RPE in suspension.

Discussion

In the present study we showed that a GA-like phenotype can be induced and maintained long-term in the large-eyed rabbit by subretinal bleb injection of PBS or $NaIO_3$. We further

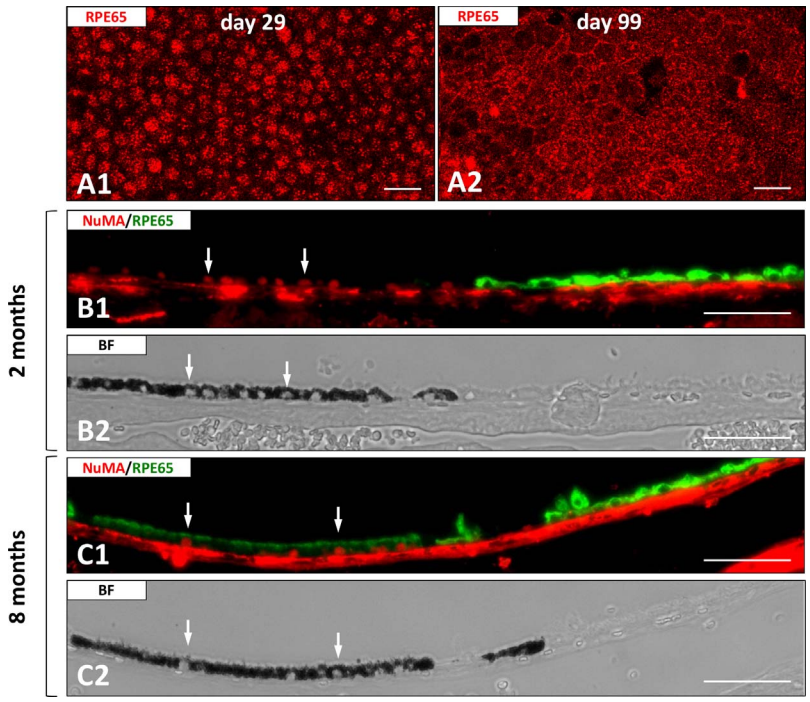

Figure 3. RPE65 expression of native and hESC-derived RPE. Immunostaining of cultured hESC-RPE for RPE65 through time (**A**). Nonpigmented native RPE are strongly positive for RPE65 in vivo (**B**, **C**). NuMA-positive hESC-RPE transplanted in suspension integrated as a pigmented subretinal monolayer (**B**, **C**). Staining of hESC-RPE for RPE65 is negative after 2 months, yet becomes positive after 8 months. BF, bright field. *Scale bars*: (**A**) 20 μm; (**B**, **C**) 50 μm.

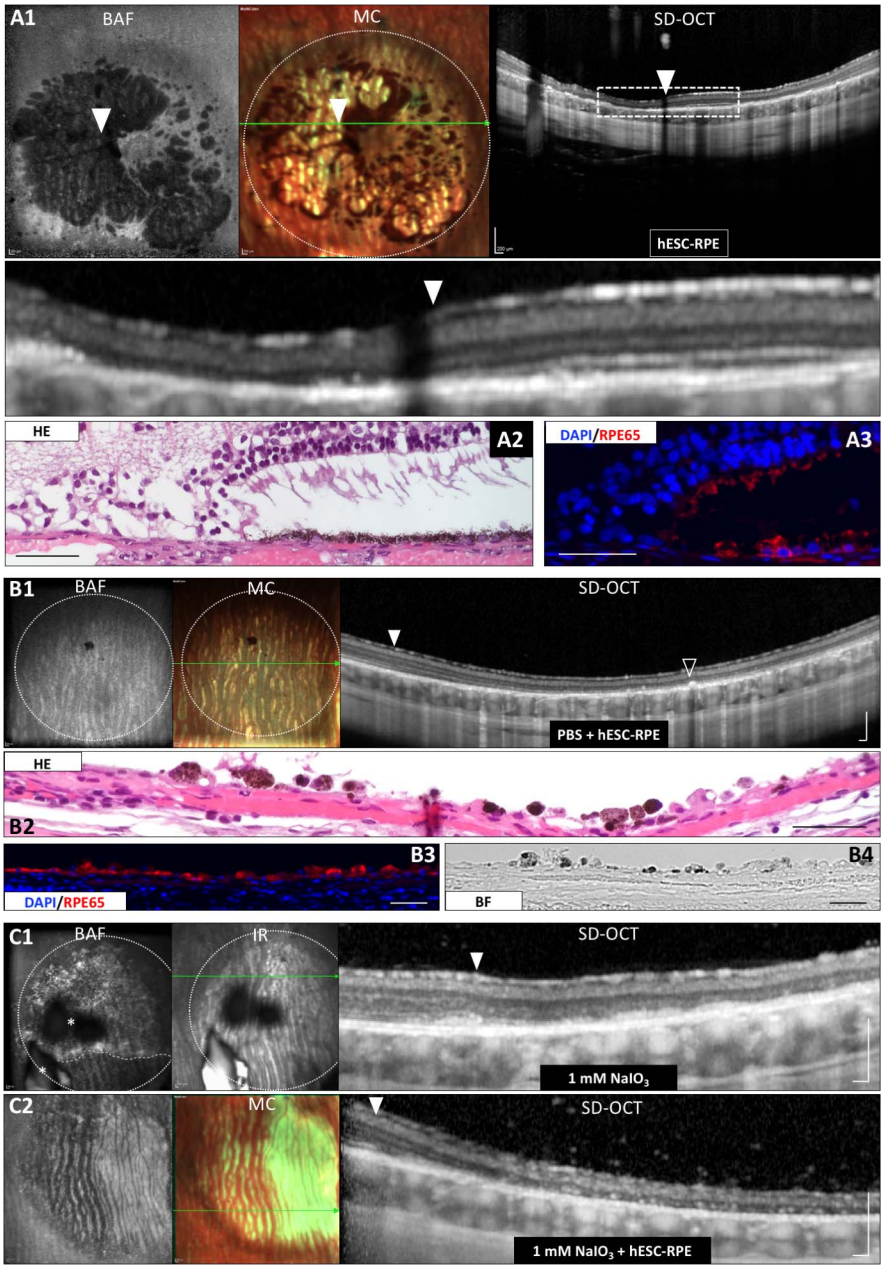

Figure 4. Transplantation of hESC-RPE in naive and PBS- or $NaIO_3$-pretreated eyes. Subretinal transplantation of hESC-RPE in suspension (*dotted circle*) into nonpretreated naive albino rabbits shows patchy areas of pigmentation in eyes with injection-induced native RPE loss (**A1**). Large RPE denuded hypo-BAF areas are present 3 months after transplantation. On the corresponding multicolor cSLO image, pigmented areas are seen between bright atrophic areas. On SD-OCT, the neuroretina overlying the area with integrated hESC-RPE is well-preserved, in contrast to the adjacent area denuded of native RPE that shows outer retinal layer loss extending to the inner plexiform layer. The transition between the native RPE-denuded and hESC-RPE integrated area is marked (*arrowhead*), and the corresponding box magnified below. The SD-OCT scan plane is marked (*green arrow*). Hematoxylin and eosin (**A2**) and immunostaining (**A3**) for RPE65 demonstrates loss of native RPE adjacent to the integrated and weakly RPE65-positive hESC-RPE. Also note the striking difference in outer neuroretinal preservation between these areas. Suspension transplantation of hESC-RPE 1 week after pretreatment of the same area with PBS (*dotted circle*) showed presence of pigmented subretinal dots (*open arrowhead*) on multimodal imaging after 3 months (**B1**). Hematoxylin and eosin (**B2**) and immunostaining for RPE65 [**B3**], corresponding bright field image [**B4**]) demonstrated occasional pigmented RPE-like cells exhibiting an abnormal morphology in the subretinal space. When eyes were pretreated with 1 mM $NaIO_3$ for 1 week (**C1**) followed by hESC-RPE transplantation, no pigmented areas were detected after 3 months (**C2**). In addition, the neuroretina overlying the transplanted area showed extensive atrophy. The margins of the bleb (*closed arrowhead*) and the SD-OCT scan planes are marked (*green arrow*). A hypo-BAF area is also outlined (*dashed line* in [**C1**]) where intravitreal triamcinolone particles (*asterisks*) partially block the BAF and IR signals. IR, infrared scanning laser ophthalmoscopy; MC, multicolor scanning laser ophthalmoscopy. *Scale bars*: (**A1**, **B1**, **C1**, **C2**) 200 μm; (**A2**, **A3**) 50 μm; (**B2**, **B3**, **B4**) 20 μm.

Table 3. Integration of Transplanted hESC-RPE

Pretreatment	Eyes Included, *n*	Integration, *n**	Trace, *n*†	No Integration, *n*‡	RPE Atrophy, *n*§
None	14	5	6	3	NA
PBS	5	0	2	3	1
$NaIO_3$	5	0	0	5	5

* Pigmented area >2.5 mm^2.
† 0.0 mm^2 $<$ pigmented area $<$ 2.5 mm^2.
‡ Pigmented area $= 0.0$ mm^2.
§ Area of hypo-BAF detected before transplantation. NA, not applicable.

presented preclinical evidence that subretinal suspension transplants of hESC-RPE cannot properly integrate in eyes with GA-like degeneration.

Extending on our previous observation that subretinal PBS causes highly reproducible photoreceptor degeneration in the rabbit,[12] we have presented long-term data further suggesting that such changes are irreversible. We have speculated that the mechanism for this is related to the merangiotic retina of the rabbit that renders the retina entirely dependent on the underlying choroidal vasculature for oxygenation.[18] Thus, a subretinal bleb that temporarily induces retinal hypoxia may be sufficient to cause photoreceptor death. The mechanism of PBS-induced RPE loss (i.e., hypo-BAF areas) probably is different since subretinal blebs do not detach the RPE, suggesting that choroidal support for the RPE remains intact. Therefore, it is more likely that the RPE loss is caused by the injection itself, possibly through random mechanical disruption of the apical villi on the RPE. In support, we found PBS-induced RPE loss to be a rare and mostly limited event. Interestingly, the neuroretina overlying areas of hypo-BAF (i.e., RPE loss) showed further atrophy compared to adjacent areas overlying the hyper-BAF zone. This suggested that RPE loss accentuates neuroretinal cell death, a conclusion further supported by the $NaIO_3$ data. As described before, bleb-induced hyper-BAF is highly reproducible and correlates with an abnormal RPE mosaic.[12] In the present study, these RPE were found to maintain normal morphology and RPE65 expression. Nevertheless, BAF increased through time, implying gradual accumulation of intracellular fluorophores as evidence of progressive structural RPE damage.

Subretinal $NaIO_3$ induced dose-dependent outer neuroretinal degeneration and RPE loss. These results essentially confirmed previous observations using systemically administered $NaIO_3$, for which the morphologic and molecular effects have been characterized extensively in rabbit and rodent models.[15–17] Early ultrastructural studies in rabbit demonstrated the first retinal changes to occur in the RPE already after 7 to 10 hours with subsequent photoreceptor swelling and degeneration.[15] Later studies have shown that lower doses of $NaIO_3$ cause patchy RPE loss whereas higher doses lead to widespread RPE loss within 1 week.[19,20] The effects on the neurosensory retina also have been explored, describing either formation of photoreceptor cell rosettes or homogenous degeneration of the outer nuclear layer.[17,20] Recently, it was further shown that photoreceptors and RPE die through distinct mechanisms, the former through apoptosis and the latter through necroptosis.[21] In a swine model, subretinal blebs of $NaIO_3$ were shown to induce dose-dependent damage to the outer neuroretina and alterations to the RPE/Bruch's complex as shown by SD-OCT.[22] However, since BAF was not used in that study, a direct comparison at the RPE level with the present study cannot be done.

Albeit the previously stated, a question remains regarding the faithfulness of PBS- or $NaIO_3$-induced damage in mimicking clinical GA. On SD-OCT, clinical GA is characterized by degeneration of the outer neuroretinal layers, the RPE/Bruch complex, and the choriocapillary/choroidal layer.[6,23,24] The RPE changes can be analyzed further by BAF, where the end-stage areas of cell loss become hyporeflective and the surrounding border of viable cells become hyperreflective.[25,26] In the present study, we have shown that subretinal PBS or $NaIO_3$ induce many GA characteristic changes. Overall, PBS-induced changes were milder mimicking an earlier disease phenotype with loss of photoreceptor layers on SD-OCT and hyper-BAF of the RPE. By contrast, $NaIO_3$-induced changes relate closer to end-stage GA, including more extensive loss of outer retinal layers and hypo-BAF areas of RPE loss. In addition, we found evidence of $NaIO_3$-induced choroidal atrophy. We concluded that subretinal PBS/$NaIO_3$ blebs in the rabbit induce damage that realistically captures most of the pathology of clinical GA. Thus, it is a relevant preclinical model for investigating the rejuvenating capacity of hESC-RPE.

As we have shown previously, hESC-RPE derived by our xeno-free and defined protocol become heavily pigmented during in vitro differentiation.[13] Following subretinal transplantation, the cells initially become depigmented, whereafter pigmentation reappears after approximately 1 month. By analyzing RPE65 expression through time, we found a similar pattern further demonstrating that hESC-RPE undergo a phase of de- and rematuration when transferred from in vitro to in vivo conditions. Analysis of factors that regulate and optimize in vivo maturation of transplanted hESC-RPE merits further study.

In this study, we have confirmed and extended our previous finding that subretinal transplants of hESC-RPE in suspension can form extensive functional monolayers.[13] We were specifically interested in whether hESC-RPE could integrate in eyes with preinduced GA-like degeneration using either PBS or $NaIO_3$. Under these conditions, occasional donor cells with abnormal morphology were detected following PBS but not $NaIO_3$ pretreatment, presenting evidence of poor integration in eyes with damage to the outer neuroretina/RPE complex. In support, integrated hESC-RPE also were not found in areas with outer retinal degeneration and native RPE loss of nonpretreated naive eyes. It should be noted that the failure of hESC-RPE to integrate in the present study may be a consequence of the unique features of the rabbit eye, the nature of the induced degeneration (using PBS or $NaIO_3$) in addition to the immunosuppression regiment (intravitreal triamcinolone). Nevertheless, our results suggested that hESC-RPE in suspension can integrate properly only if the subretinal milieu is sufficiently preserved.

Xenografts of hESC-RPE are expected to trigger an immunologic response if the outer blood–retina barrier is compromised. In our previous study, we occasionally noted subretinal infiltration, choroidal swelling, and absence of pigmented donor cells, which we suggested to be signs of xenogenic rejection.[13] This is supported further by preliminary histologic analysis demonstrating that the subretinal infiltrates represent mononuclear cells (data not shown). In the present study, we found signs of possible immunorejection in PBS- or $NaIO_3$-pretreated transplanted eyes. Pretreated areas were

injected twice; thus, increasing the risk of mechanical disruption of the outer blood–retina barrier that in turn may have triggered an immune response. This observation underscores the importance of addressing the risk of immunorejection when transplanting hESC-RPE into pathologic eyes.

Despite the surgical difficulties and putative immunologic response to the transplant, implantation of sheets of hESC-RPE with or without a supportive biomatrix may be more efficient in repopulating areas with more extensive damage to the outer neuroretina/RPE/Bruch's membrane complex.[9,27,28] However, preclinical results in large-eyed animals suggest that caution is warranted, as such constructs may cause outer retinal atrophy.[10,28] Therefore, it would be important to optimize this technology, if successful integration of hESC-RPE is to be achieved in areas of extensive atrophy.

Taken into a clinical context the presented preclinical data suggest that suspension transplants of hESC-RPE may have the capacity to functionally repopulate the area outside the GA but not the GA area itself. In agreement, preliminary data from the first clinical trial on hESC-RPE showed presence of pigmented tissue at the border of the atrophic area in GA patients.[1,29] Therefore, for the suspension approach to be functionally effective, it will most likely be crucial to choose patients diagnosed in an early stage of the disease, with a relatively conserved outer retina. The large-eyed GA model presented in this study should be a valuable tool for further understanding if and when hESC-RPE-based treatments may succeed in a clinical setting.

Acknowledgments

The authors thank Linnea Tankred for assistance in animal care.

Supported by grants from the Karolinska Institute, the Crown Princess Margareta's Foundation for the Visually Impaired, the Edwin Jordan Foundation for Ophthalmological Research, the Swedish Eye Foundation, the King Gustav V Foundation, the ARMEC Lindeberg Foundation, and the Cronqvist Foundation.

Disclosure: **S. Petrus-Reurer**, None; **H. Bartuma**, None; **M. Aronsson**, None; **S. Westman**, None; **F. Lanner**, None; **H. André**, None; **A. Kvanta**, None

References

1. Schwartz SD, Regillo CD, Lam BL, et al. Human embryonic stem cell-derived retinal pigment epithelium in patients with age-related macular degeneration and Stargardt's macular dystrophy: follow-up of two open-label phase 1/2 studies. *Lancet*. 2015;385:509–516.
2. Song WK, Park K-M, Kim H-J, et al. Treatment of macular degeneration using embryonic stem cell-derived retinal pigment epithelium: preliminary results in Asian patients. *Stem Cell Reports*. 2015;4:860–872.
3. Idelson M, Alper R, Obolensky A, et al. Directed differentiation of human embryonic stem cells into functional retinal pigment epithelium cells. *Cell Stem Cell*. 2009;5:396–408.
4. Lund RD, Wang S, Klimanskaya I, et al. Human embryonic stem cell-derived cells rescue visual function in dystrophic RCS rats. *Cloning Stem Cells*. 2006;8:189–199.
5. Bhutto I, Lutty G. Understanding age-related macular degeneration (AMD): relationships between the photoreceptor/retinal pigment epithelium/Bruch's membrane/choriocapillaris complex. *Mol Aspects Med*. 2012;33:295–317.
6. Kvanta A, Casselholm de Salles M, Amrén U, Bartuma H. Optical coherence tomography of the foveal microvasculature in geographic atrophy [published online ahead of print August 16, 2016]. *Retina*. doi:10.1097/IAE.0000000000001248.
7. Curcio CA, Johnson M. Structure, function, and pathology of Bruch's membrane. In: Ryan SJ, Schachat AP, Wilkinson CP, Hinton DR, Sadda SR, Wiedemann P. *Retina, 5th Edition*. Elsevier Inc.; 2013:465–481.
8. Sugino IK, Sun Q, Wang J, et al. Comparison of fRPE and human embryonic stem cell-derived RPE behavior on aged human Bruch's membrane. *Invest Ophthalmol Vis Sci*. 2011;52:4779–4997.
9. Diniz B, Thomas P, Thomas B, et al. Subretinal implantation of retinal pigment epithelial cells derived from human embryonic stem cells: improved survival when implanted as a monolayer. *Invest Ophthalmol Vis Sci*. 2013;54:5087–5096.
10. Stanzel BV, Liu Z, Somboonthanakij S, et al. Human RPE stem cells grown into polarized RPE monolayers on a polyester matrix are maintained after grafting into rabbit subretinal space. *Stem Cell Reports*. 2014;2:64–77.
11. Kvanta A, Grudzinska MK. Stem cell-based treatment in geographic atrophy: promises and pitfalls. *Acta Ophthalmol*. 2014;92:21–26.
12. Bartuma H, Petrus-Reurer S, Aronsson M, Westman S, André H, Kvanta A. In vivo imaging of subretinal bleb- induced outer retinal degeneration. *Invest Ophthalmol Vis Sci*. 2015;56:2423–2430.
13. Plaza Reyes A, Petrus-Reurer S, Antonsson L, et al. Xeno-free and defined human embryonic stem cell-derived retinal pigment epithelial cells functionally integrate in a large-eyed preclinical model. *Stem Cell Reports*. 2016;6:1–9.
14. Rodin S, Antonsson L, Niaudet C, et al. Clonal culturing of human embryonic stem cells on laminin-521/E-cadherin matrix in defined and xeno- free environment. *Nat Commun*. 2014;5:3195–3208.
15. Grignolo A, Orzalesi N, Calabria GA. Studies on the fine structure and the rhodopsin cycle of the rabbit retina in experimental degeneration induced by sodium iodate. *Exp Eye Res*. 1966;5:86–97.
16. Wang J, Iacovelli J, Spencer C, Saint-Geniez M. Direct effect of sodium iodate on neurosensory retina. *Invest Ophthalmol Vis Sci*. 2014;55:1941–1952.
17. Yang Y, Ng TK, Ye C, et al. Assessing sodium iodate-induced outer retinal changes in rats using confocal scanning laser ophthalmoscopy and optical coherence tomography. *Invest Ophthalmol Vis Sci*. 2014;55:1696–1705.
18. Prince JH. *The Rabbit in Eye Research*. Springfield, IL: Charles Thomas; 1964.
19. Franco LM, Zulliger R, Wolf-Schnurrbusch UEK, et al. Decreased visual function after patchy loss of retinal pigment epithelium induced by low-dose sodium iodate. *Invest Ophthalmol Vis Sci*. 2009;50:4004–4010.
20. Carido M, Zhu Y, Postel K, et al. Characterization of a mouse model with complete RPE loss and its use for RPE cell transplantation. *Invest Ophthalmol Vis Sci*. 2014;55:5431–5444.
21. Hanus J, Anderson C, Sarraf D, Ma J, Wang S. Retinal pigment epithelial cell necroptosis in response to sodium iodate. *Cell Death Discovery*. 2016;2:16054.
22. Monés J, Leiva M, Pena T, et al. A swine model of selective geographic atrophy of outer retinal layers mimicing atrophic AMD: A phase 1 escalating dose of subretinal sodium iodate. *Invest Ophthalmol Vis Sci*. 2016;57:3974–3983.
23. Göbel AP, Fleckenstein M, Schmitz-Valckenberg S, Brinkmann CK, Holz FG. Imaging geographic atrophy in age-related macular degeneration. *Ophthalmologica*. 2011;226:182–190.
24. Forte R, Querques G, Querques L, Massamba N, Le Tien V, Souied EH. Multimodal imaging of dry age-related macular degeneration. *Acta Ophthalmol*. 2012;90:E281–E287.

25. Delori FC, Dorey CK, Staurenghi G, Arend O, Goger DG, Weiter JJ. In vivo fluorescence of the ocular fundus exhibits retinal pigment epithelium lipofuscin characteristics. *Invest Ophthalmol Vis Sci*. 1995;36:718–729.
26. Holz FG, Bindewald-Wittich A, Fleckenstein M, et al. Progression of geographic atrophy and impact of fundus autofluorescence patterns in age-related macular degeneration. *Am J Ophthalmol*. 2007;143:463–472.
27. Kamao H, Mandai M, Okamoto S, et al. Characterization of human induced pluripotent stem cell-derived retinal pigment epithelium cell sheets aiming for clinical application. *Stem Cell Reports*. 2014;2:205–218.
28. Ilmarinen T, Hildenmaa H, Kööbi P, et al. Ultrathin polyimide membrane as cell carrier fort subretinal transplantation of human embryonic stem cell derived retinal pigment epithelium. *PLoS One*. 2015;10:e0143669.
29. Schwartz SD, Tan G, Hosseini H, Nagiel A. Subretinal transplantation of embryonic stem cell-derived retinal pigment epithelium for the treatment of macular degeneration: An assessment at 4 years. *Invest Ophthalmol Vis Sci*. 2016;57: ORSFc1–ORSFc9.

Investigative Ophthalmology & Visual Science